

archi|DOCT

*The e-journal for the
dissemination of doctoral
research in architecture.*

Supported by the ENHSA Network | *Fueled by the* ENHSA Observatory



9

July 2017

www.enhsa.net/archidoct

ISSN 2309-0103

**PROTOTYPING STRUCTURES
IN ARCHITECTURE**

Shell structure: Analysis of hyperbolic paraboloid in paper

Ana Laura Rocha Peña // Polytechnic University of Catalonia-Barcelona Tech

Abstract

In contrast to the opinion of many people, who think that technology will eliminate paper, tons of paper are used daily worldwide. The annual average paper consumption is 48 kg per person, which is equivalent to approximately 347,035,970.30 tons. In the last few years the architect Shigeru Ban has motivated research in the field of paper as building material. In this paper, we evaluate the implementation of paper as building material in shell structures. At first, paper does not seem to be strong enough to be used as structural material, however we propose shaping it, in order to improve its structural behavior. We have simulated a hyperbolic paraboloid (HYPAR) of paper in Abaqus software based on the finite element method (FEM), and analyzed its structural behavior. The analysis results demonstrate the feasibility of using paper as building material.

Keywords

Shell structure, Paper as building material, Hyperbolic paraboloid, Form optimization.

Note

This essay is the result of an extensive research conducted for the author's Master Thesis at the Polytechnic University of Catalonia-Barcelona Tech (UPC), completed in October 2016. Due to the complexity of the calculations of the HYPAR, we first calculated a plate by using the Navier method. Then, we compared these results with those obtained from a simulation model of the same plate in Abaqus. Likewise, we use this model as reference to compare it with a HYPAR structure and made a comparative analysis between paper and concrete, since concrete is a material well known and by now, widely studied.

Introduction

Shell structures are constructed systems described by three-dimensional curved surfaces, in which one dimension is significantly smaller compared to the other two. They are form-passive and resist external loads, predominantly through membrane stresses. A shell transfers external loads to its supports predominantly through forces acting in the plane of the shell surface, which are called membrane stresses. The shell surface is normally stressed in compression, or in combined compression and tension. A 'thin' shell has to be sufficiently 'thick' to carry these compressive stresses without buckling. Shell structures can be constructed as a continuous surface or from discrete elements following that surface. Geometric shapes such as sections of spheres, hyperbolic paraboloids and regular polyhedrals are also commonly used.

The challenge is to find geometries that can work entirely in compression under gravity loading. These geometries are not limited only to masonry, but are often built of any material. However, for traditional masonry structures, the dominant load is often due to the self-weight of the structure, and the applied live loads, with smaller effect, due to wind or snow (Adriaenssens, *et al.*, 2014).

The antecedents of shell structures are founded in Gothic architecture evolving from the heavy brick vaults to the slender and ribbed vaulted alloys. The most direct precedent in time is the barrel vaults. These consisted of several layers of fine brick, the first of which is placed with the help of small wooden guides and is overlaid with plaster paste, constituting a collaborative formwork. This sheet reproduces the shape of the inner curve of the vault, the following layers are superimposed. One of the most important developments in shell structures was the application of reinforced concrete. At the end of the Second World War (1945), due to lack of steel, reinforced concrete favored the development of molds with its ability to work in compression and traction, as well as to provide monolithic construction.

The construction of reinforced concrete shells became a process of study, experimentation and innovation, whereas respective contributions made by Eugène Freyssinet, Eduardo Torroja and Felix Candela were decisive (Carceles Garralón, 2007) (Figure 1).

Paper as Building Material

The first cultures to use paper as building material were the Chinese and Ancient Egyptian ones. At the beginning, it was used in form of papier-mâché, followed by the development of papyrus by the 2nd century B.C. By the 9th century A.D., the Japanese culture started to use paper elements in the construction of sliding doors and walls, called shoji-fusuma. That was the first time, when paper was utilized as an interior building component. France was the first to use paper in furniture production in the 19th century, and later as wall covering, introducing for the first time in history paper as a decorative element.

Paper products were being used in the production of aircraft and tank components in World War I. When realized that aluminum had problems with expansion and shrinking, the substitute for aluminum sheeting on aircraft wings came in form of plaster-made molds for shaping and cellulose reinforced sheets of paper combined with starch or similar adhesives. By 1920's, paper and cardboard started to be used as electrical insulation in the United States. In the same period impregnation experiments began with the introduction of cellulose fiber laminates in industry. First, phenolic-resin was used, until the development of melamine resins led to an increased popularity of paper and

cardboard as building material.

In following decades, several architects began to experiment with paper as structural material. The first building principally constructed out of cardboard was 'The 1944 House' that was followed by a period of slow development in the field. Several architects have influenced the progress of cardboard applications in architecture, with the two most influential figures, Buckminster Fuller in 1950's and Japanese architect Shigeru Ban, most recently (Sekulic, 2013) (Figure 2).

Geometry Definition

Among different shell structural configurations, a hyperbolic paraboloid was selected for the simulation. This is an anticlastic surface, whereas the center of curvature is located on opposite sides of the surface. In this type of structure, normal loads are transferred to its surface by tangential stresses (compression in the convex curve and traction in the concave curve).

The hyperbolic paraboloid equation can be written as:

$$z=kxysin(\omega)$$

Where k is a constant representing the unitary warpage of the paraboloid; $k = AA' / (OB \cdot OH \cdot \sin \omega)$. Then x and y are axes that will only be perpendicular in the case when $a = b$ and in this case, ω shall be equal to 90° .

Another way to understand this surface is to consider it as generated by a main parabola P_1 moving parallel to itself along another main parabola P_2 . Thus the surface has two systems of paraboloid generatrices (Oliva Quecedo, *et al.*, 2011).

Paper Mechanical Properties

There are three significant factors, which determine the mechanical properties of paper: The properties of fibers, the interfiber bonding and the geometrical disposition of the fiber (Figure 3). It's important to know how these factors influence the properties of paper. In laboratories, when sheets are produced for experiments, even if these have the same composition as machine produced ones, they do not have the same properties, because paper properties do not depend only on the composition, but also on the production process. Laboratory prepared paper is different than machine prepared paper (Sekulic, 2013).

Stiffness Values of Paper

Table I contains a collection of directly measured values of the elastic stiffness parameters for a few paper grades. Many values are missing, because of measurement difficulties caused by the small thickness of paper. Various estimation schemes have been developed to avoid direct measurements.

The table demonstrates that the ZD (Z-direction) stiffness of paper is generally low compared to the in-plane values. The negative value of the Poisson ratio ν_{xz} for the paperboard shows that uni-axial tensile loading in MD (machine direction) increases with thickness. In compression, at least, the elastic moduli, perhaps even the Poisson ratios, are usually equal to the corresponding tensile values. In general, the density of paper is between 300 and 900 kg/m³. The elastic modulus usually increases



Figure 1.

Los Manantiales restaurant, Félix Candela



Figure 2.

Japan Pavilion, Expo 2000 Hannover, Germany by Shigeru Ban

with density and ranges from 1000–9000 MPa, when the effect of anisotropy is removed by averaging over MD and CD (Cross-machine direction) (Niskanen, 2011).

Simulation Process

Analysis Parameters

Following the geometry exploration process, a hyperbolic paraboloid was chosen for the prototype design. For the simulation, an initial model was used starting from a quadrilateral of 6000 x 6000 mm, with height of 5000 mm, and thickness varying from 60 to 10 mm.

We have simulated the hyperbolic paraboloid of paper in Abaqus software based on FEM (Abaqus, 2004), in order to investigate its mechanical behavior (Figure 4). To this model, two general analyses (linear and nonlinear) have been conducted. A static linear analysis provides a first approximation of the structure's behavior, by considering equilibrium of the system without deformation. For obtaining precise results with regard to the response of the structure, a second-order analysis is required that incorporates the effects of material and geometry nonlinearity. The nonlinear analysis considers the properties of the material, the surface loads and the boundary conditions. All elements are assigned with an elastic modulus of 5420 MPa and a Poisson's ratio of 0.38, selected from the table of measured values of elastic stiffness (Niskanen, 2011). A uniform vertical load of 1 kN (0.001 N/m²) is applied to the surface. As to the boundary conditions, two of the four nodes are pinned with zero displacement.

Development of the Analysis

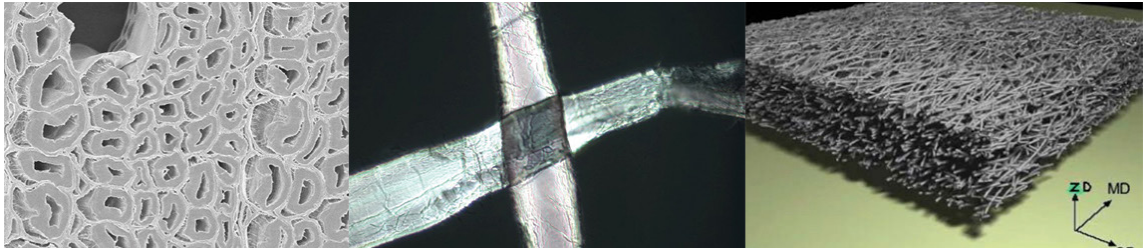
The development of the simulation model provides information about the physical behavior of the Hypar structure in paper. In all cases, the maximum deformation and the maximum stress by Von Mises in the center of the Hypar have been registered. Probably the most important properties of structural materials are their strength and stiffness. The limit stress refers to the maximum strength value of the material. The type of paper chosen for the analysis has a maximum strength value of 5.00 MPa. Currently no standard regulations exist with regard to paper as building material. We have chosen a maximum deformation limit of L/100, i.e. 8485/100= 85 mm.

To calculate the longest distance of the system, the following equation applies:

$$L_{max}=L.\sqrt{2}$$

where L is a side of the quadrilateral that makes the Hypar.

Only maximum values of the stress and deformation in the center of the Hypar have been considered in the analyses, and any respective results superior to the limits set were dismissed. For better comprehension, the analysis process is divided in three stages. The first stage, static linear analysis, considers the equilibrium of the structure without deformation. Then a second stage, static nonlinear analysis, takes into account effects of the deformed geometry. And finally, a third stage, plastic nonlinear analysis, considers effects of nonlinearity of the geometry and the material behavior.

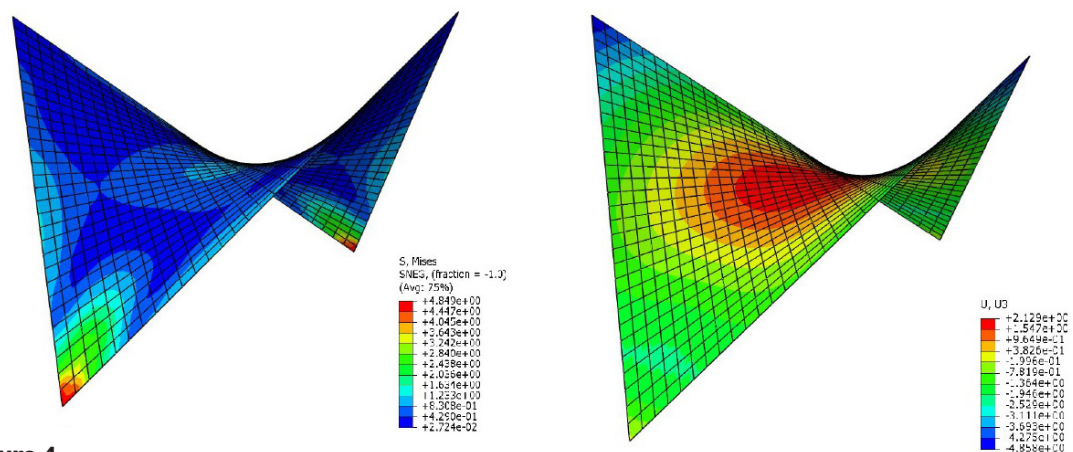
**Figure 3.**

Wood fibers, interfiber bonding and geometrical disposition of the fiber

Table I.

Measured values of elastic stiffness parameters in tensile loading for some machine made papers (Niskanen, 2011)

| | Paperboard (Persson, 1991) | Carton (Baum, 1987) | Linerboard (Baum, 1987) | Coated paper, middle of web (Stalme, 2006) | Coated paper, web edge (Stalme, 2006) |
|------------------------------|-------------------------------|------------------------|----------------------------|--|---|
| Density, Kg/m ³ | 640 | 780 | 691 | 1140 | 1140 |
| MD Modulus E_x , MPa | 5420 | 7440 | 7460 | 7690 | 7660 |
| CD Modulus E_y , MPa | 1900 | 3470 | 3010 | 3050 | 2570 |
| ZD Modulus E_z , MPa | 17 | 40 | 29 | | 140 |
| Poisson ratio ν_{xy} | 0.38 | 0.15 | 0.12 | 0.33 | 0.27 |
| Poisson ratio ν_{xz} | -2.20 | 0.008 | 0.011 | | |
| Poisson ratio ν_{yx} | 0.14 | | | 0.07 | 0.10 |
| Poisson ratio ν_{yz} | 0.54 | 0.021 | 0.021 | | |
| Poisson ratio ν_{zx} | 0.05 | | | | -0.04 |
| Poisson ratio ν_{zy} | 0.05 | | | | 0.03 |
| Shear modulus G_{xy} , MPa | 1230 | 2040 | 1800 | 1910 | 1820 |
| Shear modulus G_{xz} , MPa | 8.8 | 137 | 129 | | |
| Shear modulus G_{yz} , MPa | 8.0 | 99 | 104 | | |

**Figure 4.**

Simulation model, visualization of the Von Mises stress and deformation

Stage 1 – Static Linear Analysis

The initial model was ideal for obtaining a first approximation of the Hypar behavior. As shown in Figure 5, the highest stresses develop at the ground supports areas and the center of the Hypar on both sides (superior and inferior). This is due to the fact that the shell transfers the external loads to its supports through forces acting in plane of its surface. For the specific analysis, the resulting stress values in the center of the Hypar have been registered.

Figure 6 summarizes the Von Mises stresses in the center of the Hypar obtained from the static linear analysis. Based on the analysis conducted, the maximum stress increases with thickness reduction, even above the material strength limit.

The specific Hypar structure works along one axis as an arc and along the other axis as a suspended arc. While compression stresses tend to deform the membrane along one axis, traction stresses along the other axis, tend to counter this deformation. For this reason, the maximum deformation develops in the center of the Hypar as shown in Figure 7. Figure 8 summarizes the maximum deformations obtained from the static linear analysis. Two systems have higher deformations than the respective limit set.

Stage 2 – Static Nonlinear Analysis

The difference between linear and nonlinear analysis is the system's stiffness. When a structure deforms under an external load, it is the stiffness that changes due to the geometry or the material properties. This second stage of nonlinear analysis comprises a static nonlinear analysis that considers the system's deformation effects. In Figure 9, the results of the simulation model are presented. The last two systems do not converge.

Figure 10 summarizes the Von Mises stresses in the center of the Hypar obtained from the static nonlinear analysis. The last two models with 20 and 10 mm thickness do not converge.

As shown in Figure 11 the maximum deformations develop in the center of the Hypar. Two of the six systems do not converge.

Figure 12 summarizes the deformations obtained from the static nonlinear analysis. The last two systems with 20 and 10 mm thickness do not converge. The other four systems develop favorable results within the respective allowable limits set.

Stage 3 – Plastic Nonlinear Analysis

Finally, for obtaining most accurate results, mostly similar to reality, with regard to the Hypar structural behavior, a plastic nonlinear analysis has been conducted. The analysis at this stage considers both, the effects of nonlinearity with regard to the geometry and the material. Figure 13 shows the results of the simulation models.

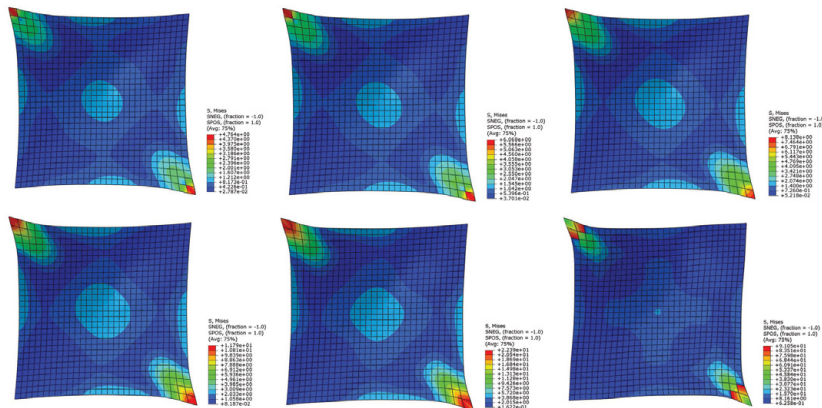


Figure 5.

Results of the simulation model - Von Mises stress in static linear analysis

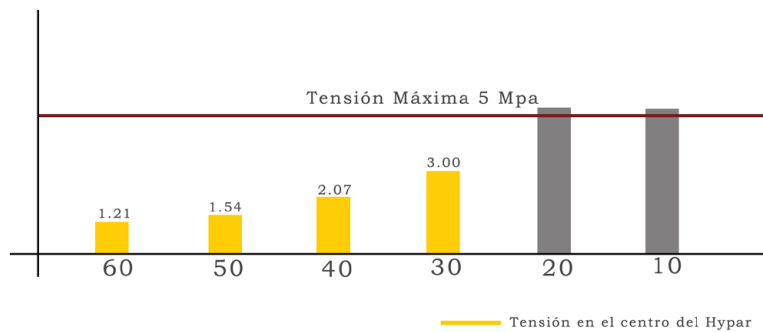


Figure 6.

Structural response - Von Mises stress in the center of the Hypar based on static linear analysis

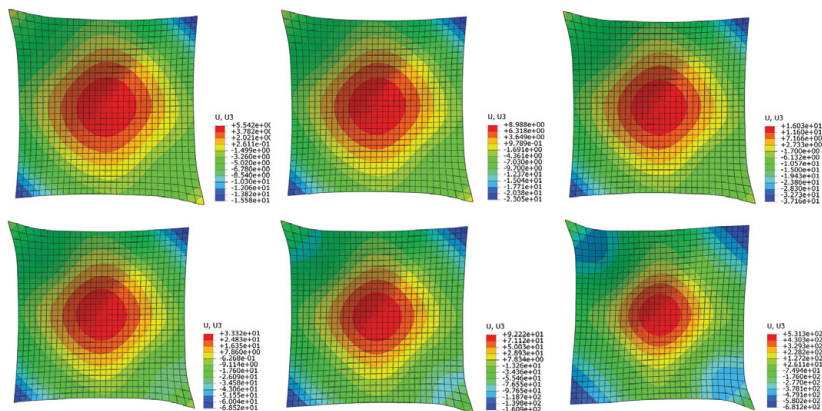


Figure 7.

Results of the simulation model - Deformation in static linear analysis

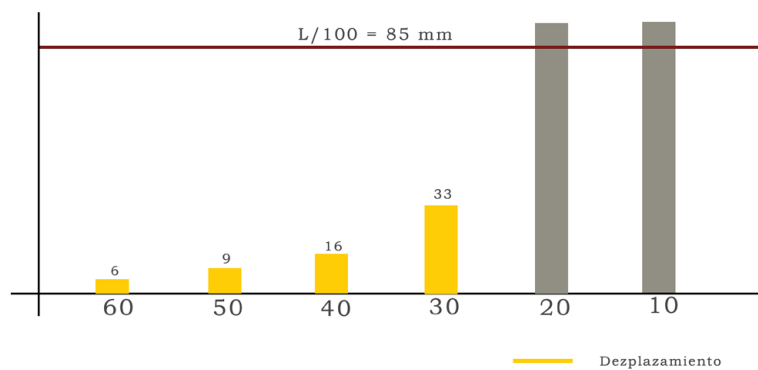


Figure 8.

Structural response - Deformation in the center of the Hypar based on static linear analysis

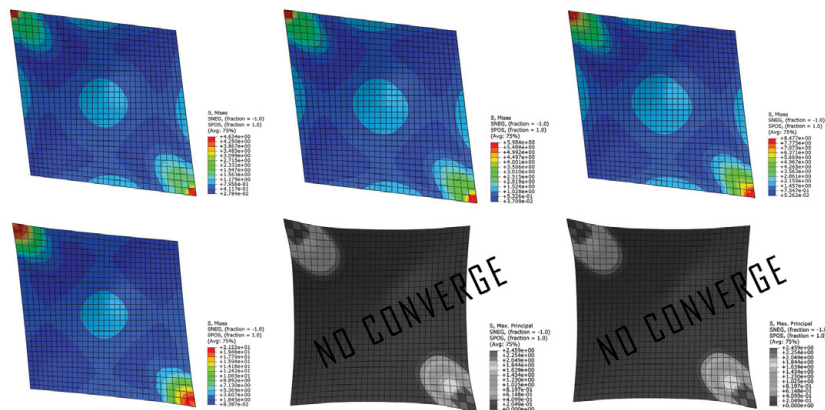


Figure 9.

Results of the simulation model - Von Mises stress in static nonlinear analysis

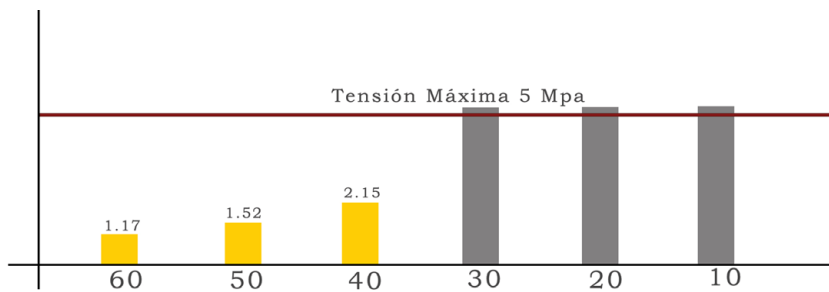


Figure 10.

Structural response - Von Mises stress in the center of the Hypar based on static nonlinear analysis

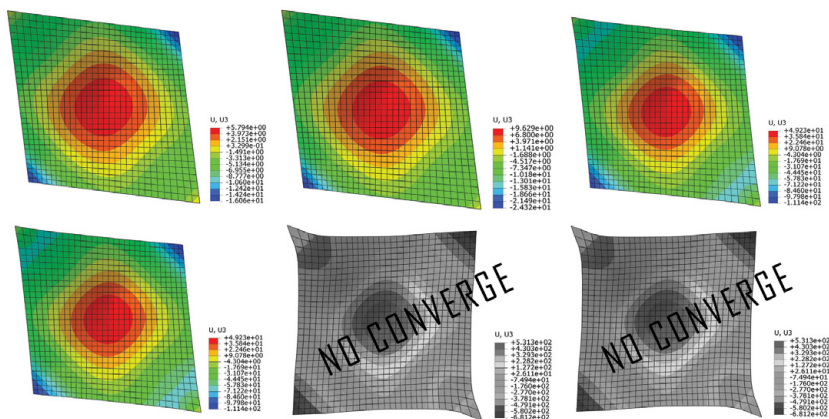


Figure 11.

Results of the simulation model - Deformation in static nonlinear analysis

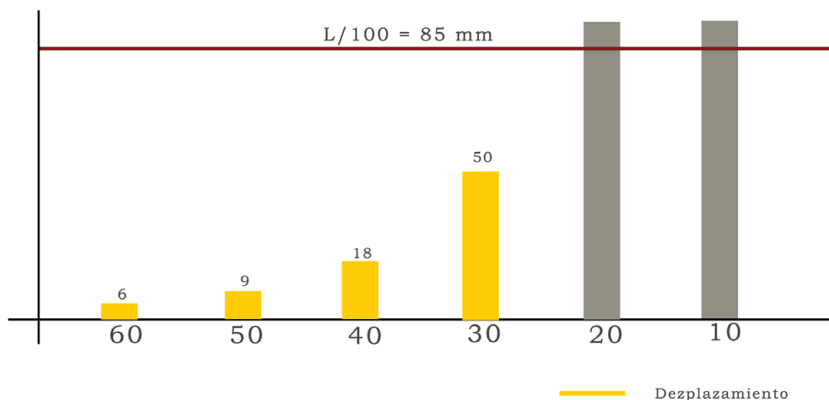


Figure 12.

Structural response - Deformation in the center of the Hypar based on static nonlinear analysis

Dezplazamiento

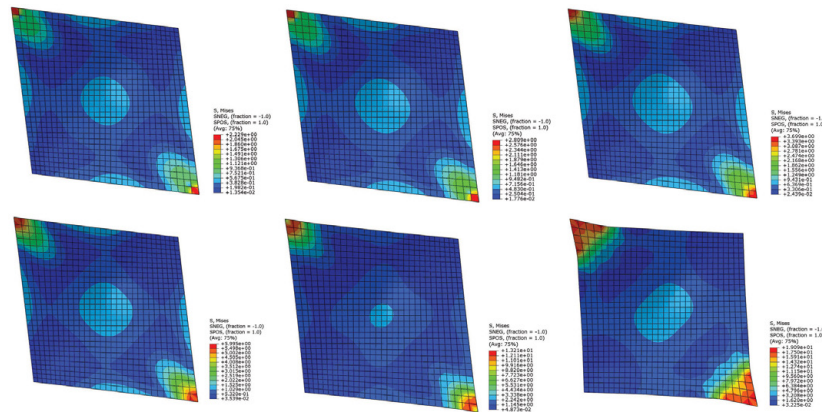


Figure 13.

Results of the simulation model - Von Mises stress in plastic nonlinear analysis

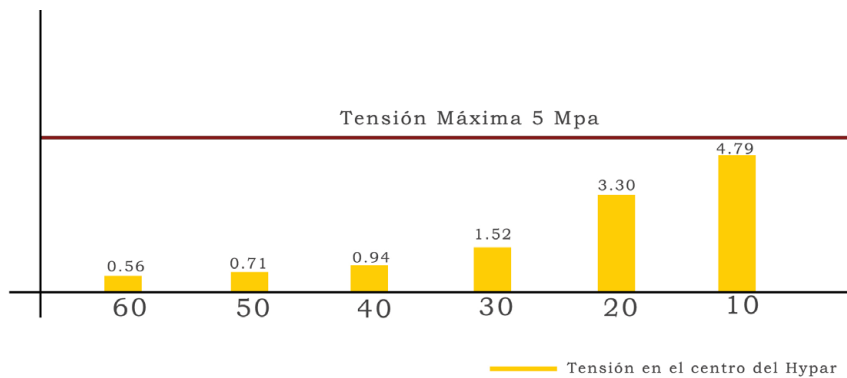


Figure 14.

Structural response - Von Mises stress in the center of the Hypar based on plastic nonlinear analysis

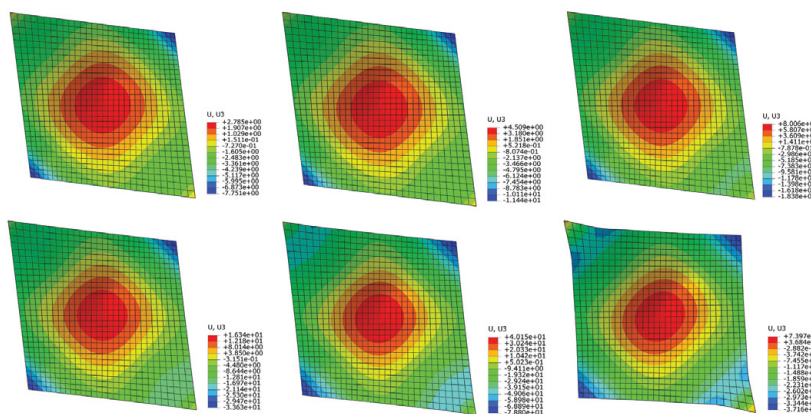


Figure 15.

Results of the simulation model - Deformation in plastic nonlinear analysis

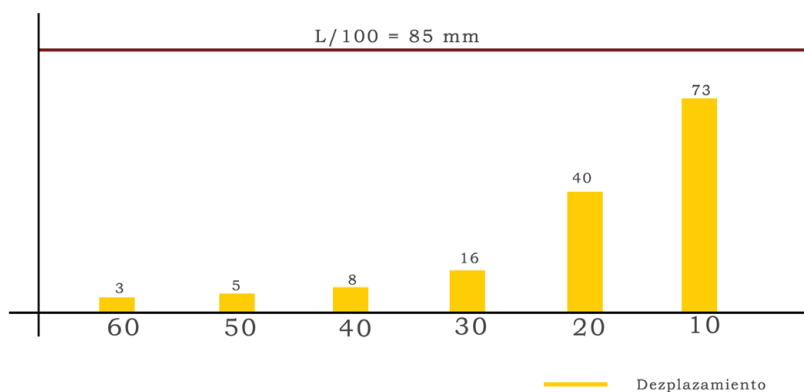


Figure 16.

Structural response - Deformation in the center of the Hypar based on plastic nonlinear analysis

Figure 14 summarizes the Von Mises stresses in the center of the Hypar obtained from the plastic nonlinear analysis. In this particular stage, all simulation systems show favorable results within the allowable limits set.

The maximum deformation of the systems develops in the center of the Hypar, as shown in Figure 15.

Figure 16 summarizes the deformations obtained from the plastic nonlinear analysis. None of the systems exceeds the allowable limits set.

Conclusions

Research activities in the field of paper as building material have increased in the last years. Paper is an excellent material with regard to providing innovative, new ways of application in construction. This material can be used as structural material for construction and as formwork of complex structures, in both cases, offering opportunities for sustainably and economically sensitive designs.

Following analyses of a hyperbolic paraboloid based on FEM, the following can be concluded: In a first stage of a static linear analysis, as well as in a second stage of a static nonlinear analysis considering deformation effects, the response values obtained are almost in the range of the allowable limits set in the analysis, except for the models with 20 and 10 mm thickness that have passed these limits. Finally, in a plastic nonlinear analysis, most similarly to reality, the results obtained are all favorable and within the allowable limits set. The developed stresses of the models obtained values within the range of 0.56 to 4.79 MPa, all below the respective maximum strength of the material of 5.00 MPa. All system maximum deformations are less than $L/100$, starting from 3 mm for 60 mm surface thickness and reaching 73 mm for 10 mm thickness. Therefore, the results obtained from these three stages of analyses, favor implementation of paper as building material in shell structures. Future research will investigate the mechanical behavior of the different types of paper; ways for increase of the strength of paper in combination with glued composites, of reduction of the humidity of paper, and among others, the fiber of paper as material for the 3D-printer.

References

- ABAQUS, 2004. *ABAQUS keywords: Reference Manual: Versión 6.5*. West Lafayette: ABAQUS Inc.
- Adriaenssens, S., Block, P., Veenendaal, D. and Williams, C., 2014. *Shell Structures for Architecture : Form-finding and Optimization*. London : Routledge.
- Carceles Garralón, F., 2007. *El paraboloide hiperbólico comogenerador inagotable en las estructuras laminas*. E.U. de Arquitectura Técnica (UPM).
- Niskanen, K., 2011. *Mechanics of Paper Products*. Berlin: De Gruyter.
- Oliva Quecedo, J., Antolin Sanchez, P., Cámara Casado, A. and Goicolea Ruigómez, J.M., 2011. *Análisis estructural de algunas obras de Félix Candela mediante modelos de Elementos Finitos*. Hormigón y Acero. E.T.S.I. Caminos, Canales y Puertos (UPM).
- Sekulic, B., 2013. *Structural Cardboard: Feasibility Study of Cardboard as a Long-term Structural Material in Architecture*. Universitat Politècnica de Catalunya.